

# ANALYSIS OF INVERTER CHARGING WAVEFORM FOR ULTRA STABLE SCSS MODULATOR

Jong-Seok Oh<sup>1,2,#</sup>, Takahiro Inagaki<sup>1</sup>, Katsutoshi Shirasawa<sup>1</sup>, Tsumoru Shintake<sup>1</sup>  
<sup>1</sup>RIKEN Harima Institute, <sup>2</sup>PAL/POSTECH.

## Abstract

The SCSS (SPring-8 Compact SASE Source) XFEL [1] requires ultra stable RF sources. The SCSS smart modulator driving a klystron RF source uses an inverter charging system. Therefore, the stability of RF sources is directly determined by the one of inverter power supplies. The regulation and the stability of an inverter depend on not only the structure of inverter topology but also the fidelity of a signal monitoring. For better stability, we need stable and adequate monitoring of a charging voltage. The charging waveform is composed of a net PFN (pulse forming network) voltage and ripple components that is related to the system-dependent circuit parameters. This ripple is proportional to the ratio of the PFN capacitance to the stray capacitance of a pulse transformer and a klystron load. We can manipulate the feedback signal with suitable filtering but it is shown that the charging stability depends on the way of signal conditioning also. The long-term drift has to be minimized by the temperature stabilization of the probe and feedback circuits.

## INTRODUCTION

The SCSS XFEL uses normal conducting technology for beam acceleration, in which pulse-to-pulse power fluctuation in RF-system dominates beam stability. The RF output is mainly fluctuating due to the pulse-to-pulse variation of a klystron voltage that is determined by the PFN charging voltage of a modulator. The inverter is responsible to the RF stability because it charges the PFN capacitor. In order to stabilize the charging level, we need a clean and stable signal for the PFN voltage. There are not only pulse forming network capacitors but also protective series resistors and distributed reactive components of a pulse transformer and a klystron load in the charging path. Therefore, the charging waveform becomes somewhat complicated. The understanding of the charging waveform and the proper conditioning of feedback signal is necessary to realize an ultra stable charging performance. This paper shows the detail analysis of the charging waveform of SCSS modulators and the stability dependency on the signal conditioning.

## SCSS MODULATOR

Figure 1 shows the circuit topology and its charging waveform for inverter charging scheme using a constant current source. This scheme is compared with the ones of the traditional resonant charging scheme using a constant voltage source. The inverter topology provides high reliability: a thyatron switch is safely turned off because

next charging schedule is digitally controllable, it is inherently fail-safe system under short-circuit condition due to the current limit feature of a constant current power supply. In addition, it is naturally compact by using a high frequency inverter. Also it has other attractive features: expandability, easy maintenance, and flexible control interface [2]. These features are well matched to the next generation modulator for SCSS XFEL facility.

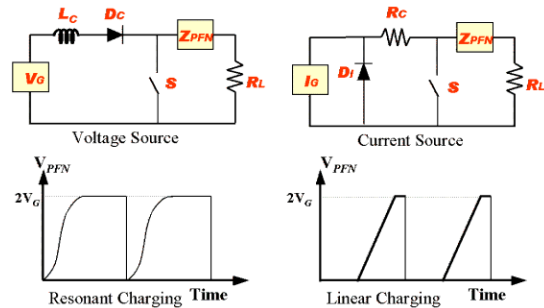


Figure 1: Basic circuits and charging waveforms of a voltage source and a current source power supply.

Figure 2 shows the simplified circuit diagram of SCSS modulator that consists of a PFN, a thyatron switch, a pulse transformer, and an inverter power supply as a PFN charging unit. The inverse voltage is limited by a tail circuit absorbing the magnetic energy stored in the pulse transformer. The main specifications are as follows; 114-MW peak power, 30-kW average power, 60-pulse per second, 3.8- $\mu$ s pulse width, 1:16 step-up ratio, 350-kV peak voltage (secondary side) [3].

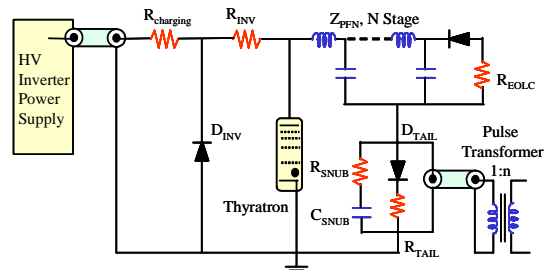


Figure 2: Simplified circuit diagram of SCSS modulator.

Figure 3 shows detailed charging waveforms of a C-band modulator ( $C_{PFN} = 0.4 \mu F$ ) around the charging level of 38 kV. The average increment of charging step  $\Delta V_{PFN}$  is about 100 V with a switching frequency  $f$  of 34.6 kHz; therefore, the average charging current  $I_{dc}$  is 1.38 A at this charging level according to the following equation.

$$I_{dc} = C_{PFN} \Delta V_{PFN} f \tag{1}$$

#jsoh@postech.ac.kr

The charging voltage is not rising smoothly and monotonically but includes high-frequency spikes. The magnitude of spikes is larger than the increment of charging level for each switching cycle. The voltage waveform at the pulse transformer secondary shown in the figure has similar oscillating pattern. Therefore, it is expected that the spike is made by the circuit components connected in parallel to the pulse transformer. The noisy spikes seem to be harmful for the feedback circuit to correctly compare the charging level with a reference level.

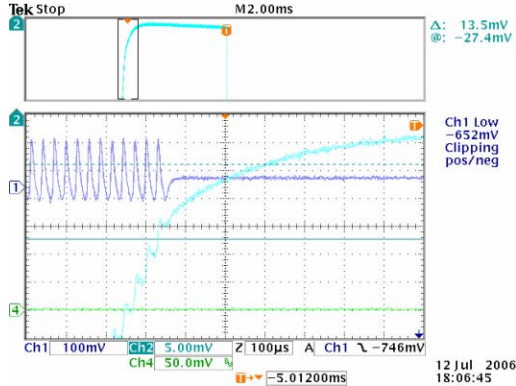


Figure 3: Waveforms of charging buckets (Upper box: charging voltage waveform, Lower box: expanded view of square box marked on the upper box for pulse transformer secondary voltage (upper curve, 1.18 kV/div) and PFN charging voltage (lower curve, 100 V/div), Horizontal: 100 μs/div)

### ANALYSIS OF CHARGING WAVEFORM

In order to analyze the circuit response of charging current, it is useful to know the Fourier components of charging current. The inverter output is a full-wave rectified current as shown in Figure 4.

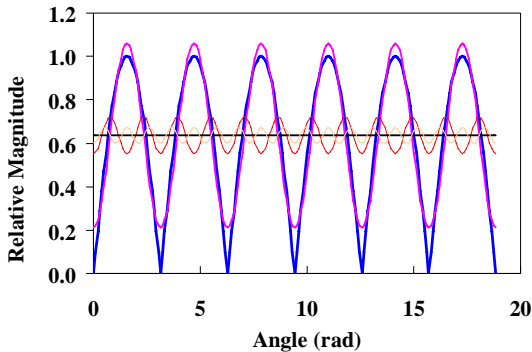


Figure 4: Full-wave rectified current (thick blue line) and Fourier series.

It has an average value of  $I_{dc}$  and higher frequency components  $I_{ac}$ . The average current is  $2/\pi$  of a peak value  $I_{peak}$ . The second harmonic current is dominant and it is  $4/(3\pi)$  of the peak value according to Eq. (2). Therefore, the magnitude of second harmonic current is 66.7% of the average charging current;  $I_{ac} = (2/3) I_{dc}$ .

$$\begin{aligned} \frac{I_{ac}}{I_{peak}} &= -\frac{4}{\pi} \sum_{n=2}^{\infty} \frac{\cos n\omega t}{(n+1)(n-1)} \quad (n = \text{even only}) \\ &= -\frac{4}{\pi} \left[ \frac{1}{3} \cos 2\omega t + \frac{1}{15} \cos 4\omega t + \dots \right] \approx -\frac{4}{3\pi} \cos 2\omega t \end{aligned} \quad (2)$$

The output current from an inverter power supply,  $I$ , has to flow through the series impedances of  $R_1$ ,  $R_2$ ,  $Z_{PFN}$ , and  $Z_L$  in the equivalent charging circuit shown in Figure 5. The charging current flows through the complicated load impedance network  $Z_L$ . The spike voltage is generated by oscillation caused by the total stray capacitance and the magnetizing inductance of a pulse transformer.

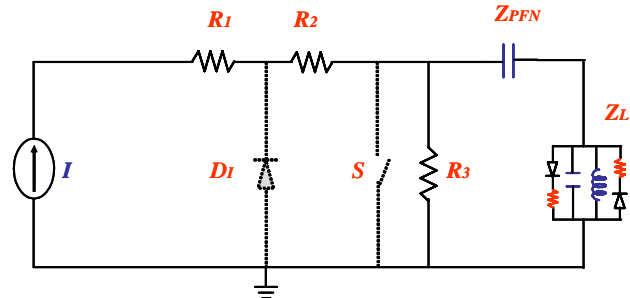


Figure 5: Equivalent charging circuit.

To improve the present stability of SCSS modulators, it is planned to use an ultra stable inverter power supply that is operating in parallel with a main inverter. The concept and design example is described in Ref. [4]. This inverter has small charge per switching with higher switching frequency. The frequency response of the charging network of a SCSS modulator measured because of the possibility of a resonance, which distorts the charging waveform. Figure 6 shows the measured data and the calculated frequency response by the circuit model. The phase transition occurs at 40 kHz that is caused by the parallel resonance driven by the magnetizing inductance  $L_{mag}$  of a pulse transformer and total stray capacitance  $C_{stray}$  of a pulse transformer and a klystron load. Series resonance at higher frequency of Figure 6-(b) is driven by  $C_{stray}$  and a series inductance in the charging path.

The second harmonic current of a SCSS modulator is capacitive-coupled because its frequency is higher than 40 kHz. There is no resonance till 250 kHz and the gain is monotonically decreasing. Therefore, higher frequency is able to be applied without serious waveform distortion for a high precision inverter up to 100 kHz.

The ripple voltage,  $V_{ac}$  introduced by the second harmonic current through a stray capacitive impedance  $X_c$  ( $=2\pi f C_{stray}$ ) is given by

$$V_{ac} = I_{ac} X_c = I_{dc} / (6\pi f C_{stray}) \quad (3)$$

The ripple factor defined by  $2V_{ac} / \Delta V_{PFN}$  is the relative magnitude of the ripple voltage to the increment of a charging voltage per one cycle of an inverter switching. By using Eq. (1) and (3), the ripple factor is

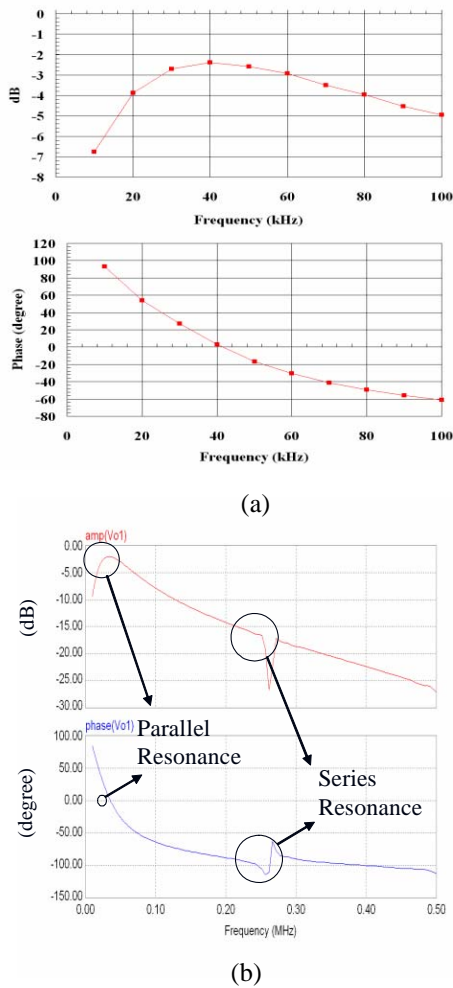


Figure 6: Frequency response of a charging network of a SCSS modulator: (a) measured data, (b) circuit simulation.

$$2V_{ac} / \Delta V_{PFN} = C_{PFN} / (3\pi C_{stray}) \quad (4)$$

Table 1 shows the summary of ripple voltage parameters for the SCSS modulator. In order to verify this evaluation, equivalent circuit analysis is performed.

Table 1: Ripple voltage parameters of charging waveform

PFN capacitance, $C_{PFN}$	0.4 $\mu$ F
Average charging current, $I_{dc}$	1.58 A
Switching frequency, $f$	34.6 kHz
Increment of charging, $\Delta V_{PFN}$	114.2 V
Stray capacitance, $C_{stray}$	25.9 nF
Ripple current, $I_{ac}$	1.05 A
Charging impedance, $X_c$	88.8 $\Omega$
Ripple voltage, $V_{ac}$	93.2 V
Ripple factor, $2V_{ac} / \Delta V_{PFN}$	1.63

Figure 7 shows the simulated charging waveform with the conditions given in the Table 1. Figure 7(a) is the initial charging waveform. The net PFN voltage (V<sub>PFN</sub>-V<sub>primary</sub>) is monotonically increasing but the PFN

voltage (V<sub>PFN</sub>) has 100-V ripple with second harmonic frequency. It shows that the DC component  $I_{dc}$  is flowing through the magnetizing inductance of a pulse transformer ( $I_{Lmag}$ ) and AC ripple current is mainly flowing through the stray capacitance ( $I_{Cstray}$ ). Figure 7(b) is the charging waveform at the 38 kV level. The former half of the full-wave rectified current is gradually increasing to two-time large value than the initial one, and the latter half is gradually decreasing to zero. Accordingly, the diode in the tail circuit is turned on as the positive primary peak is increasing. At last, it becomes half-wave rectified waveform having a two times large peak current but the net average charging current is still same.

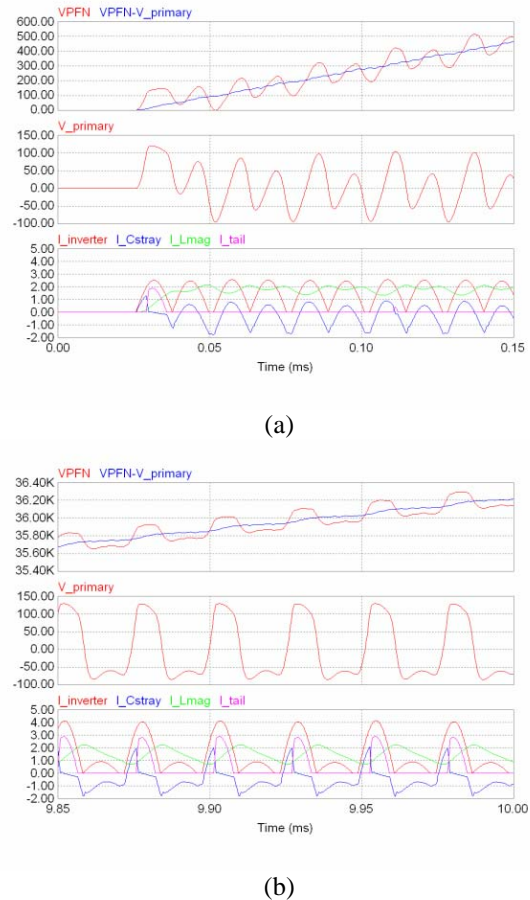


Figure 7: Simulated charging waveforms: “V<sub>PFN</sub>” = PFN voltage from ground potential, “V<sub>PFN</sub> - V<sub>primary</sub>” = net PFN voltage: (a) initial charging waveform, (b) charging waveform around 36 kV.

The Fourier series of the higher harmonic for the half-wave rectified waveform depicted in Figure 8, is described by

$$\begin{aligned} \frac{I_{ac}}{I_{peak}} &= \frac{1}{2} \sin \omega t - \frac{2}{\pi} \sum_{n=2}^{\infty} \frac{\cos n \omega t}{(n+1)(n-1)} \quad (n \text{ even only}) \\ &= \frac{1}{2} \sin \omega t - \frac{2}{\pi} \left[ \frac{1}{3} \cos 2\omega t + \frac{1}{15} \cos 4\omega t + \dots \right] \quad (5) \end{aligned}$$

The dominant term now has same frequency as the switching one and its magnitude is 50% of the average

charging current that is similar to the one of dominant term for the full-wave rectified waveform. Therefore, its ripple has same magnitude as the one of full-wave mode.

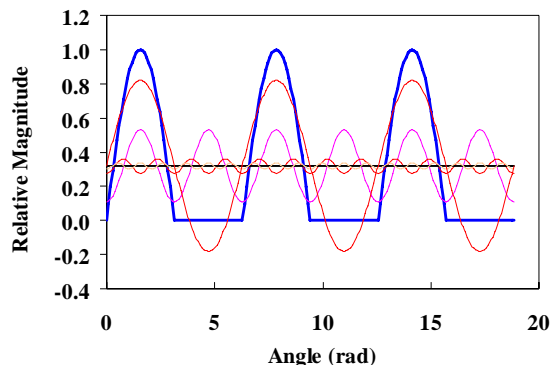


Figure 8: Half-wave rectified current (thick blue line) and Fourier series.

### EFFECT OF SIGNAL FILTERING

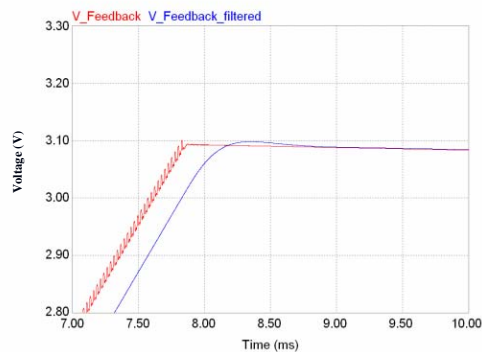
The charging voltage is determined by the command reference. The reference level is compared with a feedback signal coming from a high voltage probe. Therefore, not only the reference level but also the feedback signal has to have high fidelity and stability. Figure 9 shows how improper conditioning of monitoring signal affect the charging stability under the reference level of 30 kV. The high frequency ripple on the rising slope of a feedback signal is well filtered out in the case (a); 1-kHz low pass filter. The charging voltage is regulated at the level higher than the reference one. Therefore, it is not able to correct the time dependent variation of the droop of top level. If the circuit has low frequency cut below 0.5 Hz, then, the actual PFN voltage is gradually rising even the comparator circuit is feeling the same level of feedback signal as shown in the case (b).

### SUMMARY AND DISCUSSION

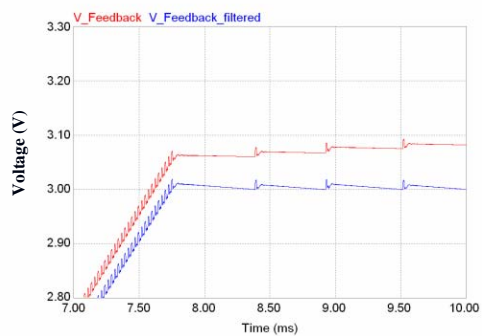
The SCSS modulator has many features fitting to the XFEL application, which are provided by adopting the inverter power supply that is one of governing factors for the stability of electron beams of SCSS linac. The ripple voltage superimposed on the PFN charging waveform is analyzed as a function of circuit parameters. It is found that the ripple factor is proportional to the ratio of the PFN capacitance to the stray capacitance. The conditioning of the feedback signal has large effect on the regulation of PFN voltage. The understanding of the charging waveform and the proper conditioning of feedback signal is essential to realize an ultra stable charging performance.

It is possible to measure the net differential voltage by using an additional probe that has equally calibrated and balanced for high frequency response.

The high voltage components of a probing system such as resistors and capacitors are temperature sensitive elements. The devices on the low level feedback circuits



(a)



(b)

Figure 9: Regulation characteristic for different filtering of a feedback signal with high voltage probe attenuation of 1/10,000: (a) 1 kHz low pass filter, (b) 0.5 Hz high pass filter.

also have thermal drift. Therefore, it is essential to stabilize the temperature of the probe and feedback circuits to remove the long-term slow drift of beam energy.

### REFERENCES

- [1] <http://www-xfel.spring8.or.jp>
- [2] J. S. Oh, et. al., "Development and Application of an Inverter Charging Supply to a Pulse Modulator," the XXI International LINAC Conference, Korea, 2002.
- [3] T. Inagaki, et. al., "High Power Test of the Compact, Oil-Filled Modulator for C-band Klystron," the third Asian Particle Accelerator Conference, Korea, 2004.
- [4] J. S. Oh, et. al., "Development of an Ultra Stable Klystron-Modulator for PAL XFEL," the 27<sup>th</sup> International Free Electron Laser Conference, USA, 2005.